

Critical Magnetic Scattering of Neutrons by Iron

H. A. GERSCH, *Georgia Institute of Technology, Atlanta, Georgia*

AND

C. G. SHULL* AND M. K. WILKINSON, *Oak Ridge National Laboratory, Oak Ridge, Tennessee*

(Received April 26, 1956)

The experimental results of Wilkinson and Shull for the small-angle magnetic scattering of 0.9 Å neutrons from iron at temperatures close to the Curie point are analyzed in terms of the instantaneous correlation between pairs of spins of the iron atoms. Fourier inversion of the angular distribution of the scattering gives the spatial dependence of the spin-spin correlations, while their temperature dependence follows from the temperature variation of the angular distributions. The correlation functions so obtained are compared with the asymptotic form predicted by statistical mechanics and show consistency with the measured values of the paramagnetic susceptibility for iron above the Curie temperature.

I. INTRODUCTION

THE experimental results presented in the previous paper for the small-angle magnetic scattering of about 1 Å neutrons from iron in the vicinity of the Curie temperature appear to be a manifestation of fluctuation phenomenon peculiar to macroscopic systems in the vicinity of critical points. The general features of these fluctuations were recognized a long time ago in experimental and theoretical studies¹ of the abnormally large scattering of light from dense gases in the vicinity of their critical points (the so-called critical opalescence). Since that time much work has been done on the small-angle x-ray scattering from dense gases.²

The interpretation of the small-angle magnetic neutron scattering in terms of fluctuations in magnetic moment density and range of correlations between spins is closely analogous to the interpretation of the small-angle x-ray scattering in terms of fluctuations in particle density and range of the molecular pair distribution function. This connection, established in detail by Van Hove,³ is another example of the close analogy between the two systems, others being the similarity with regard to thermodynamic variables as well as to specific statistical models.⁴ Some qualitative aspects which bear on the scattering properties of both systems near critical points will now be mentioned.

In these studies, the essential point is that one has to deal with cooperative systems, in which the elements of the system cooperate to form units, and in which the ability to form such units depends markedly on the extent to which the elements have already cooperated. For the gas, the cooperation is insured by the attractive part of the intermolecular forces which cause the forma-

tion of clusters, while for the ferromagnet, there are the exchange interactions between neighboring atoms that give rise to a coupling energy which depends on the spins of neighboring atoms and which allows formation of clusters of aligned spins.

Knowledge of the intermolecular forces between gas particles determines (at least in principle) the probability distribution for finding a particle at any distance from a given one. Similarly, the spin-dependent energy of the ferromagnet determines the probability for finding the spins surrounding a given one aligned with it. These probability distributions determine the collective scattering properties of the system.

When the minimum potential energy between a pair of elements of the system is small compared to their thermal energy, then these probability distributions are quite closely determined by considering only the direct interaction of the pair. However, as the temperature is lowered toward a critical point, the distance and temperature dependence of the probability distributions take on a special behavior which reflects the essential cooperative nature of the effects, and which is accompanied by anomalous behavior in the thermodynamic variables of the system. This state of affairs exists in a rather small temperature region surrounding the critical temperature, and in this region, gives rise to very special scattering properties.

In Sec. II, the connection between magnetic moment fluctuations and spin-spin correlations is discussed; a formal treatment is given in Appendix I. The determination of the correlations by Fourier inversion of the experimental small-angle magnetic scattering is treated in Sec. III. These results are compared with the asymptotic form for the correlations predicted by statistical mechanics and with the observed paramagnetic susceptibility for iron in Sec. IV.

II. FLUCTUATIONS AND CORRELATIONS

The qualitative behavior of the correlations which determine the magnetic scattering properties can be inferred from a general result of statistical mechanics which connects fluctuations in magnetic moment with

* Now at Massachusetts Institute of Technology, Cambridge, Massachusetts, assigned to Brookhaven National Laboratory, Upton, New York.

¹ For a list of these, see M. J. Klein and L. Tisza, *Phys. Rev.* **76**, 1861 (1949).

² For a general discussion, see A. Guinier and G. Fournet, *Small Angle Scattering of X-Rays* (John Wiley and Sons, Inc., New York, 1955), Chap. 2.

³ L. Van Hove, *Phys. Rev.* **95**, 1374 (1954).

⁴ T. D. Lee and C. N. Yang, *Phys. Rev.* **87**, 410 (1952).

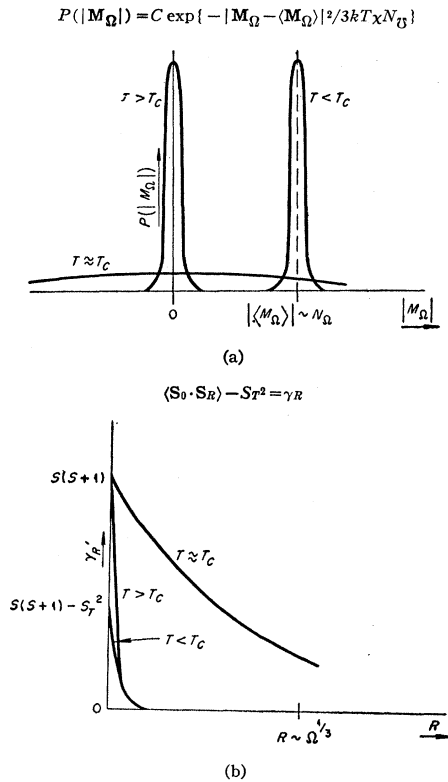


FIG. 1. Qualitative behavior of the magnetic moment fluctuations and spin-spin correlations for a ferromagnet at different temperatures. (a) Probability distribution $P(|\mathbf{M}_\Omega|)$ for magnetic moment $|\mathbf{M}_\Omega|$ of the subregion Ω at different temperatures. (b) Distance dependence of γ'_R , the deviation of the spin-spin correlation $\langle \mathbf{S}_0 \cdot \mathbf{S}_R \rangle$ from its asymptotic value S_T^2 at temperatures corresponding to those in Fig. 1(a).

magnetic susceptibility. Analogous relations for gases relating particle density fluctuations to compressibility are well known.⁵

Consider the magnetic moment \mathbf{M}_Ω of a subregion Ω of the ferromagnet, small compared to the total volume, yet containing a tremendous number of spins N_Ω . This moment is the vector sum of all the atomic magnetic moments in the subregion, and fluctuates about its average value, $\langle \mathbf{M}_\Omega \rangle$, so that an instantaneous picture of the region would, in general, show a magnetic moment different from the average. The extent of the excursions of the magnetic moment from the average value is measured by the mean square deviation from the average, $\langle |\mathbf{M}_\Omega - \langle \mathbf{M}_\Omega \rangle|^2 \rangle = \langle |\mathbf{M}_\Omega|^2 \rangle - |\langle \mathbf{M}_\Omega \rangle|^2$. Since the probability for observing a magnetic moment $M_\Omega \equiv |\mathbf{M}_\Omega|$ will be a Gaussian centered about the average value, the quantity $\{ \langle M_\Omega^2 \rangle - |\langle \mathbf{M}_\Omega \rangle|^2 \}^{1/2}$ will measure the half-width of this distribution. The qualitative temperature dependence of these probability distributions, as inferred from the following discussion, is shown in Fig. 1(a). Consider first temperatures above the Curie temperature T_c and vanishing external magnetic

field \mathbf{H} . We neglect anisotropic interactions, so that the properties of the spin lattice are invariant to simultaneous rotation of all spins. Then from the statistical mechanical definition of the average value of a dynamical variable there follows the relation

$$\langle M_\Omega^2 \rangle = 3kTN_\Omega\chi, \quad (1)$$

where $\chi = N_\Omega^{-1} \lim_{H \rightarrow 0} (\partial \langle M_\Omega \rangle / \partial H)$ is the magnetic susceptibility per spin. At temperatures above and removed from T_c , χ is well-behaved, and the half-width is proportional to the square root of the number of moments N_Ω in the subregion. From this we conclude that the chance of observing a fluctuation in magnetic moment proportional to the total number N_Ω is essentially zero. However, as T approaches T_c , the susceptibility in vanishing external magnetic field approaches ∞ (or rather χ becomes of order N_Ω which is the same thing in the limit $N_\Omega \rightarrow \infty$), and fluctuations in \mathbf{M}_Ω become tremendous. In particular, the probability of finding a fluctuation for which the magnetic moment has a value proportional to N_Ω is no longer negligible and will occur for appreciable fractions of the time of observation. This situation will exist only in the narrow temperature interval above T_c . For temperatures below T_c , the same qualitative behavior of the fluctuations is expected as T is increased toward T_c , although Eq. (1) does not hold in this region. The temperature region $T < T_c$ is characterized by the presence of spontaneous magnetization or long-range ferromagnetic order, so that as \mathbf{H} is reduced to zero, $\langle \mathbf{M}_\Omega \rangle$ tends to a finite value which increases rapidly as T decreases from T_c . For this temperature region we may choose the z axis of our coordinate system along the direction of \mathbf{H} . Then, with our assumption of isotropic spin-spin interactions, $\langle \mathbf{M}_\Omega \rangle$ will lie along this direction. A calculation similar to that involved in Eq. (1) shows that the fluctuations in the z -component of magnetic moment are given by the formula

$$\langle M_{\Omega z}^2 \rangle - \langle M_{\Omega z} \rangle^2 = kTN_\Omega\chi, \quad (2)$$

where as in Eq. (1), χ is the susceptibility per spin in vanishing magnetic field. Since χ must increase as T increases toward T_c , with $\chi \rightarrow \infty$ as $T \rightarrow T_c$, we again expect the fluctuations to become very large as T_c is approached from lower temperatures.

The qualitative behavior of the correlations between pairs of spins, which is important with regard to the small-angle magnetic scattering of neutrons, is now easy to see. We first recall the definition and significance of the correlation function. Calling \mathbf{S}_0 the spin at the (arbitrarily chosen) origin, and \mathbf{S}_R the spin at a lattice point a distance R away, the scalar correlation between the two spins is defined as the average of their product, $\langle \mathbf{S}_0 \cdot \mathbf{S}_R \rangle$. This quantity is a measure of the influence of one spin on the other, and reduces to the product of the averages $\langle \mathbf{S}_0 \rangle \cdot \langle \mathbf{S}_R \rangle = |\langle \mathbf{S}_0 \rangle|^2 \equiv S_T^2$ when R becomes very large. With ferromagnetic interactions, the two spins \mathbf{S}_0 and \mathbf{S}_R tend to be aligned, and $\langle \mathbf{S}_0 \cdot \mathbf{S}_R \rangle$ will be

⁵ See, for example, R. C. Tolman, *The Principles of Statistical Mechanics* (Oxford University Press, Oxford, 1950), Chap. XIV.

a positive decreasing function of R , tending to the limiting value S_T^2 . Since $S_T = |\langle \mathbf{S}_0 \rangle|$ is proportional to the average magnetic moment per spin at temperature T , in the absence of an external magnetic field we will have S_T equal to zero in the paramagnetic region above the Curie point. As the temperature is lowered below the Curie temperature, S_T rises rapidly, giving rise to elastic magnetic scattering localized in the diffraction peaks.

Scattering through small angles depends strongly on the correlation at large distances, so let us consider $\langle \mathbf{S}_0 \cdot \mathbf{S}_{R'} \rangle$ where R' is a distance of the order of the linear dimensions of the volume Ω previously chosen. For the ferromagnet at temperatures above and removed from T_c , $\langle \mathbf{S}_0 \cdot \mathbf{S}_{R'} \rangle$ is essentially zero. This follows from our previous conclusion that in this temperature range fluctuations with magnetic moment proportional to N_Ω almost never occur, which implies that these two spins are almost never aligned. In these small fluctuations, then, we expect to find regions over which one spin exerts an appreciable influence on its neighbors, but only over distances of the order of some few atomic spacings. If we call these regions spin clusters, we may say that the spin clusters are of atomic size when the fluctuations are normal. However, as T_c is approached from above, the existence of magnetic moments M_Ω proportional to the total number of spins N_Ω implies that these two spins, although separated by very many atomic distances, are aligned for appreciable fractions of the time. Therefore as the Curie temperature is approached, $\langle \mathbf{S}_0 \cdot \mathbf{S}_{R'} \rangle$ increases and reaches a maxi-

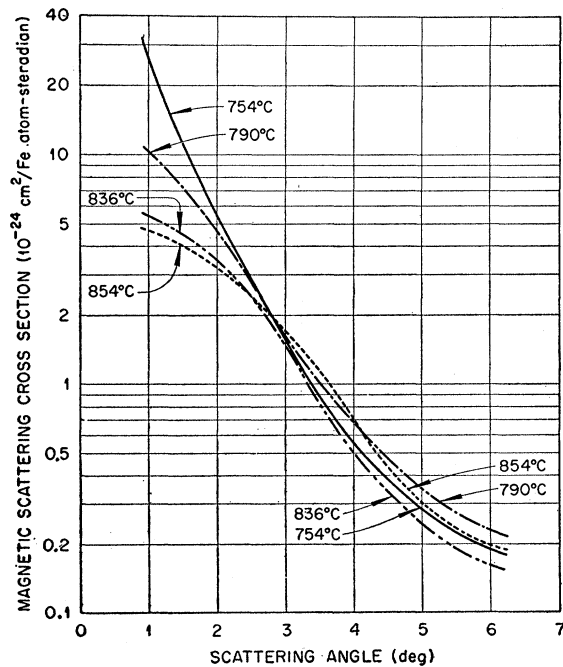


FIG. 2. Small-angle magnetic scattering of 0.9 Å neutrons produced by iron at different temperatures.

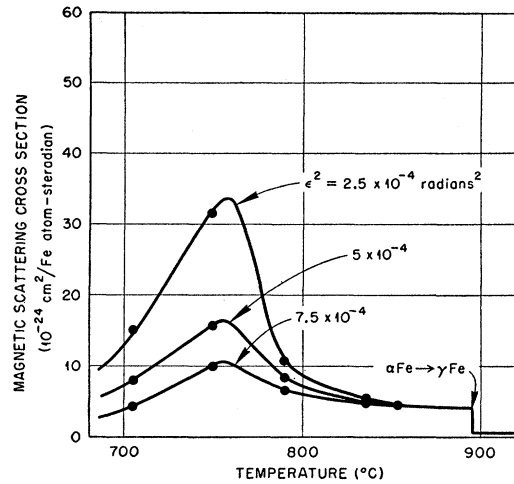


FIG. 3. Temperature variation of the magnetic scattering of 0.9 Å neutrons produced by iron at several fixed scattering angles.

mum at this temperature, where the fluctuations are the largest. The correlated regions, or spin clusters, now have a spatial extent much larger than atomic dimensions.

The above argument repeated for temperatures below T_c shows that $\langle \mathbf{S}_0 \cdot \mathbf{S}_{R'} \rangle$ must differ from its asymptotic value S_T^2 as T_c is approached from below, with the deviation becoming a maximum at T_c . A more formal development of these ideas is contained in Appendix I.

As remarked, with ferromagnetic interactions, we expect the correlation function to be a monotonically decreasing function of the separation distance R , so that its qualitative dependence on distance and temperature can be inferred from our considerations above. Figure 1, which summarizes this discussion, shows this dependence in the three different temperature regions. We may note that it is the behavior of the deviation of the spin-spin correlation function $\langle \mathbf{S}_0 \cdot \mathbf{S}_R \rangle$ at large distances from its asymptotic value S_T^2 which should be symmetric above and below T_c .

III. FOURIER INVERSION OF THE SCATTERING DATA

The angular dependence of the small-angle neutron magnetic scattering data for several temperatures is shown on an absolute scale in Fig. 2. Significant features of these curves are the greatly increased neutron scattering at the small angles over the paramagnetic value, and the sharp rise in the smallest angle scattering as the temperature is lowered toward the Curie point. Figure 3 shows the temperature variation of the magnetic scattering for several fixed scattering angles. According to our previous discussion, the behavior illustrated by these two figures implies a corresponding increase in both the magnetic moment fluctuations and the range of the correlation between a pair of spins. This spin-spin

correlation function $\langle \mathbf{S}_0 \cdot \mathbf{S}_R \rangle$ will now be obtained from Fourier inversion of the scattering data.

The differential cross section for inelastic magnetic scattering per unit solid angle and unit interval of outgoing neutron energy ϵ for a polycrystal of N spins is³

$$\frac{d^2\sigma}{d\Omega d\epsilon} = \left(\frac{\gamma e^2}{mc^2}\right)^2 \frac{N}{3\pi\hbar k_0} |f(\kappa)|^2 \sum_R \int dt \times \exp[i(\boldsymbol{\kappa} \cdot \mathbf{R} - \omega t)] \gamma_{R'}(t), \quad (3)$$

where \mathbf{k}_0 and $\mathbf{k} = \mathbf{k}_0 - \boldsymbol{\kappa}$ are initial and final wave vectors of the neutron and $\omega = \hbar(k_0^2 - k^2)/m$, m being the neutron mass, and γ is the neutron magnetic moment. Here $\gamma_{R'}(t)$ is the time-dependent deviation of the correlation function from its asymptotic value, $\gamma_{R'}(t) = \langle \mathbf{S}_0(0) \cdot \mathbf{S}_R(t) \rangle - S_T^2$. The time dependence of $\gamma_{R'}(t)$ accounts for the neutron-spin lattice energy exchanges, and permits qualitative discussion of the degree of inelasticity in terms of the spin-spin relaxation time and the time spent by a neutron in traveling over a correlation range. These energy exchanges, by no means negligible at general temperatures, become very small as the Curie point is approached. This is pointed out in Van Hove's work, where he shows that the relaxation time for the magnetic moment fluctuations becomes very large as $T \rightarrow T_c$. Under these conditions, the time the neutron spends in a correlation range is much less than the relaxation time, which is precisely the requirement for negligible energy exchange. The same behavior is implied in the picture of the large magnetic moment fluctuations which correspond to modes of excitation for the spin system with very long wavelength and hence very small energy. Semiquantitative calculations indicating negligible energy exchange for the experimental conditions we have here are given in Appendix II.

Under these conditions the momentum transfer $\hbar\boldsymbol{\kappa}$ is essentially independent of energy transfer $\hbar\omega$, so that integrating Eq. (3) over all outgoing neutron energies gives the static approximation

$$\sigma(\kappa, T) = \frac{1}{N} \frac{d\sigma}{d\Omega} = \left(\frac{\gamma e^2}{mc^2}\right)^2 \times \frac{2}{3} |f(\kappa)|^2 \sum_R \gamma_{R'}(0) \times \exp(i\boldsymbol{\kappa} \cdot \mathbf{R}), \quad (4)$$

where $\gamma_{R'}(0)$ is the instantaneous correlation whose qualitative behavior was discussed in the previous section. Equation (4) is now quite closely analogous to the differential cross section for scattering of x-rays by fluids, the major difference being that the definite spatial location of the spins requires the sum over lattice points in Eq. (4), whereas the fluids are characterized by a continuous pair distribution function. For scattering through the small angles involved here, this difference is expected to be a minor one.

If there were no interaction between spins, then for

$T > T_c$, $\gamma_{R'}(0)$ would be zero except for $R=0$, when $\gamma_{0'}(0) = S(S+1)$, and Eq. (4) would yield the paramagnetic scattering,

$$\sigma_p(\kappa) = \frac{1}{N} \frac{d\sigma_p}{d\Omega} = \frac{2}{3} \left(\frac{\gamma e^2}{mc^2}\right)^2 |f(\kappa)|^2 S(S+1). \quad (5)$$

It will be convenient to deal with the ratio of the scattering over the paramagnetic value,

$$\sigma_c(\kappa, T) = \frac{\sigma(\kappa, T)}{\sigma_p(\kappa)} = \sum_R \frac{\gamma_{R'}(0)}{S(S+1)} \exp(i\boldsymbol{\kappa} \cdot \mathbf{R}). \quad (6)$$

It is clear that the experimental small-angle scattering data shown in Fig. 2 will furnish mainly information on the behavior of $\gamma_{R'}(0)$ for large distances R . If we limit ourselves to: (a) the distance and temperature region in which the fractional change in $\gamma_{R'}(0)$ over a lattice spacing is small, and (b) the angular region for which κ is sufficiently small so that many terms in Eq. (6) make an appreciable contribution; then this sum may be replaced by an integral and $\gamma_{R'}(0)$ treated as a continuous variable. However, in order to have some means of estimating the reliability of $\gamma_{R'}(0)$ obtained in this approximation, we will proceed formally. Writing the sum in Eq. (6) as an integral using the Dirac δ function, we have

$$\sum_R \gamma_{R'}(0) \exp(i\boldsymbol{\kappa} \cdot \mathbf{R}) = \sum_R \int \gamma(\mathbf{r}) \exp(i\boldsymbol{\kappa} \cdot \mathbf{r}) \delta(\mathbf{R} - \mathbf{r}) d\mathbf{r}, \quad (7)$$

where for simplicity $\gamma(\mathbf{r})$ has been written for $\gamma_{R'}(0)$. For the δ function, we use the representation

$$\delta(\mathbf{R} - \mathbf{r}) = (2\pi)^{-3} \int \exp[i\mathbf{t} \cdot (\mathbf{R} - \mathbf{r})] d\mathbf{t}. \quad (8)$$

The result of summing over lattice points is

$$\sum_R \exp(i\mathbf{t} \cdot \mathbf{R}) = (2\pi)^3 \prod_{i=1}^3 \delta(b_i - 2\pi l_i), \quad (9)$$

where $\mathbf{t} = \sum_{i=1}^3 b_i \boldsymbol{\tau}_i$, with the $\boldsymbol{\tau}_i$ basis vectors of the reciprocal lattice, and where the l_i ($i=1, 2, 3$) are integers. Equation (7) then becomes

$$\sum_R \gamma_{R'}(0) \exp(i\boldsymbol{\kappa} \cdot \mathbf{R}) = \frac{1}{v_0} \sum_{\boldsymbol{\tau}} \int \exp[i(\boldsymbol{\kappa} - 2\pi\boldsymbol{\tau}) \cdot \mathbf{r}] \gamma(\mathbf{r}) d\mathbf{r}, \quad (10)$$

where v_0 is the volume of the crystal cell and $\boldsymbol{\tau}$ is a vector in reciprocal lattice space. Averaging over all

directions for the polycrystal, we have

$$S(S+1)\kappa\sigma_c(\kappa, T) = \frac{4\pi}{v_0} \int_0^\infty r\gamma(r) \sin\kappa r dr + \frac{2}{v_0} \sum_{\tau \neq 0} \frac{Z_\tau}{\tau} \int_0^\infty \gamma(r) \sin\kappa r \sin(2\pi\tau r) dr, \quad (11)$$

where Z_τ is the number of reciprocal lattice points at the distance τ . The lattice structure of the crystal is reflected in the sum over reciprocal lattice distances in Eq. (11). When $\gamma(r)$ has the long-range characteristic of conditions near the Curie point, $\sigma_c(\kappa, T)$ will increase not only for κ close to zero but also close to the Bragg scattering angles defined by $\kappa = 2\pi\tau$. These latter maxima are, however, considerably weakened for the polycrystal by the averaging over crystal orientations.

The experimental scattering data shown in Fig. 2 go out to a maximum angle of 6.3° , corresponding to an upper limit for κ of 0.765 \AA^{-1} , which is considerably less than $\kappa = 3.10 \text{ \AA}^{-1}$ which corresponds to the first Bragg peak. Therefore, for the distance and temperature range previously mentioned, $\gamma(r)$ should be closely determined by using only the first term in Eq. (11), giving

$$\kappa\sigma_c(\kappa, T) = \frac{4\pi}{v_0 S(S+1)} \int_0^\infty r\gamma(r) \sin\kappa r dr. \quad (12)$$

Fourier inversion of Eq. (12) yields

$$r\gamma(r) = \frac{v_0 S(S+1)}{2\pi^2} \int_0^{\kappa_m} \kappa\sigma_c(\kappa, T) \sin\kappa r d\kappa. \quad (13)$$

This last result would be exact if the upper limit κ_m were infinite. Due to the finite upper limit, we may expect some broadening out of variations in $\gamma(r)$ with distance r , but this should be a small effect since $\gamma(r)$ is expected to be monotonic and slowly varying.

The reliability of $\gamma(r)$ obtained from Eq. (13) may then be determined by using Eq. (11) to see how well the observed scattering is reproduced.

The correlations determined from Eq. (13) are shown in Fig. 4. The integrals were evaluated using a planimeter, with κ intervals chosen sufficiently small so that there were at least six values of the integrand for every half cycle of the sine function. Values of $\gamma(r)$ were determined at about 1 Å intervals out to 10 Å, and at 2 Å intervals out to 20 Å. In these calculations, the scattering cross sections were extrapolated to zero κ value from the smallest experimentally observed $\kappa = \kappa_{\min} = 0.114 \text{ \AA}^{-1}$, corresponding to scattering angle θ_{\min} of 0.9° . We are not unaware that such extrapolation could be performed using the observed susceptibility, for from Eq. (12) there follows the formula

$$\lim_{\kappa \rightarrow 0} \sigma_c(\kappa, T) = \frac{4\pi}{v_0 S(S+1)} \int_0^\infty r^2 \gamma(r) dr, \quad (14)$$

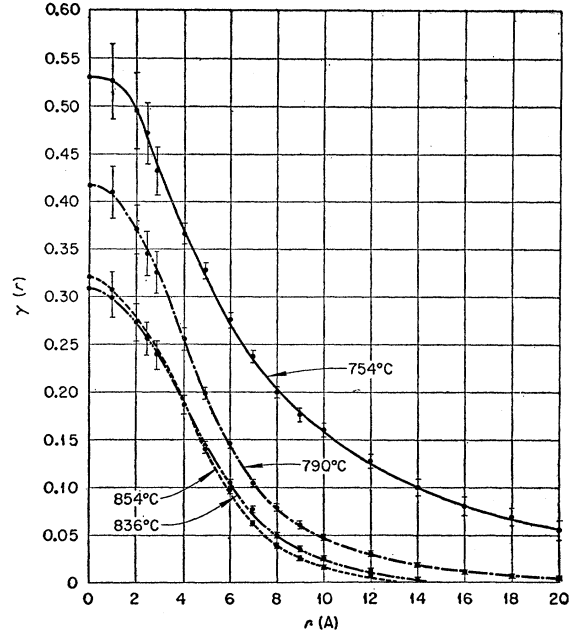


FIG. 4. Dependence of the spin-spin correlation $\gamma(r)$ on distance r at different temperatures.

while from Eqs. (A1.4) and (1) we have for $T > T_c$, the relation

$$\frac{4\pi}{v_0 S(S+1)} \int_0^\infty r^2 \gamma(r) dr = \frac{\langle M_\Omega^2 \rangle}{4\beta^2 N_\Omega S(S+1)} = \chi/\chi_1, \quad (15)$$

where χ is the observed susceptibility at the given temperature and χ_1 is the paramagnetic susceptibility $\chi_1 = (2\beta)^2 S(S+1)/3kT$ at the same temperature. Since our principal aim is to see how well the experimental data confirm the increasing range of the correlations as the Curie temperature is approached, we have not utilized this procedure. Instead, the indeterminacy in $\gamma(r)$ caused by the possible extrapolations to zero κ value consistent with the experimental data have been calculated and these are indicated by vertical bars in Fig. 4. As expected, the uncertainty in $\gamma(r)$ caused by this extrapolation is more important for the larger distances $r \gtrsim 5 \text{ \AA}$, and negligible at the smallest distances. However, the close-in correlations themselves are not precisely determined by the small-angle scattering data. This would require utilizing the data out to larger angles as well as modifying the present approximation. The range of $\gamma(r)$ values for $r \leq 5 \text{ \AA}$ which satisfactorily reproduce, within experimental errors, the observed scattering in the reliability test described below are indicated in Fig. 4, and are the major source of indeterminacy in $\gamma(r)$ at small r values. Evident from the figure is the increased range of the correlations with approach to the Curie temperature T_c (suggested to be about 760°C from the peak in the scattering cross section as a function of temperature at fixed scattering

TABLE I. Comparison of experimental and calculated $\sigma_c(\kappa, T)$.

κ (\AA^{-1})	754°C				790°C		836°C		854°C	
	$\sigma_c(\kappa)$ $r \leq 20\text{\AA}$	$\sigma_c(\kappa)$ $r \geq 20\text{\AA}$	$\sigma_c(\kappa)$	$\sigma_c(\kappa)_{\text{exp}}$	$\sigma_c(\kappa)$	$\sigma_c(\kappa)_{\text{exp}}$	$\sigma_c(\kappa)$	$\sigma_c(\kappa)_{\text{exp}}$	$\sigma_c(\kappa)$	$\sigma_c(\kappa)_{\text{exp}}$
0.1104	85.84	-15.16	70.68	71.2	24.25	24.66	12.53	12.44	10.83	10.63
0.1564	55.45	-20.17	35.28	35.9	19.01	19.33	11.15	11.14	9.85	9.66
0.1913	34.98	-11.88	23.10	22.8	15.11	15.33	9.87	9.83	8.77	8.74
0.2207	20.90	-4.34	16.56	15.9	12.25	12.24	8.69	8.77	7.78	7.94
0.2704	5.33	3.87	9.20	9.51	8.45	8.23	6.70	6.75	6.39	6.49
0.3121	0.82	5.18	6.00	6.06	5.80	5.93	5.23	5.25	5.10	5.27
0.3827	2.24	0.94	3.18	3.20	3.42	3.49	3.10	3.18	3.29	3.53
0.4413	3.94	-2.06	1.88	1.99	2.30	2.31	1.95	1.93	2.25	2.38
0.4937	3.44	-1.93	1.51	1.34	1.74	1.61	1.29	1.17	1.54	1.58
0.5842	-0.09	0.89	0.80	0.89	1.46	1.21	0.69	0.65	0.84	0.87

angle, as shown in Fig. 3). Also evident is the expected deficiency of the small angle scattering data in determining $\gamma(0)$, which should be $\gamma(0) = 2.34$ for $S = 1.11$.

The reliability of these correlations may be checked by the extent to which they reproduce the observed scattering when inserted in Eq. (11). The results are given in Table I, where the experimental $\sigma_c(\kappa, T)$ is compared with that obtained from Eq. (12). For 754°C, $\gamma(r)$ decreases so slowly that the contribution to $\sigma_c(\kappa, T)$ from $r > 20$ Å is not negligible. These contributions were calculated by using, for $r > 20$ Å, the asymptotic expression

$$\gamma(r) = (C/r) \exp(-\kappa_1 r), \quad (16)$$

with $C = 2.09$ Å, $\kappa_1 = 2.87 \times 10^6$ cm $^{-1}$. This asymptotic expression is obtained in the next section. In Table I, $\sigma_c(\kappa, 754^\circ\text{C}, r \leq 20$ Å) and $\sigma_c(\kappa, 754^\circ\text{C}, r \geq 20$ Å) are given, and their sum compared with the experimental value. For the other temperatures, the contribution to $\sigma_c(\kappa, T)$ from $r > 20$ Å is negligible. The rather close agreement shown in the table may be taken as indicating that, within the limits mentioned above, the approximate $\gamma(r)$ values must be quite close to the actual correlations.

The comparison just made has neglected the terms in the sum in Eq. (11) with $\tau \neq 0$. From the orders of magnitude involved, it is clear that these terms can make only a very small contribution to $\sigma_c(\kappa, T)$. The smallest τ value is 0.4935 Å $^{-1}$ corresponding to the (110) Bragg reflection, so that the period of the factor $\sin(2\pi\tau r)$ for this τ is closely 2 Å, compared with a period of about 10 Å for the term $\sin\kappa r$ at the largest κ value. This coupled with the fact, evident from Fig. 4, that $\gamma(r)$ does not change much over a 2 Å interval, implies a very small contribution from the terms in Eq. (11) with $\tau \neq 0$.

These correlations have also been checked by comparing their space integral with observed values of the susceptibility χ according to Eq. (15). Details and results of the comparison are given in the following section.

IV. CORRELATION FUNCTION AT LARGE DISTANCES

In this section, we will compare the behavior of $\gamma(r)$ for r considerably larger than interatomic spacings with that predicted by statistical mechanics.

For distances large compared with interatomic spacings, and for temperatures close to the Curie point, the instantaneous correlation function $\gamma(r)$ may be determined by the method introduced by Ornstein and Zernike⁶ in their treatment of the asymptotic behavior of the molecular pair distribution function for gases near critical points. The result is, in Van Hove's notation,³

$$\gamma(r) = (4\pi r_1^2 r)^{-1} v_0 S(S+1) \exp(-\kappa_1 r). \quad (17)$$

From Eq. (15), the two lengths r_1 and κ_1^{-1} are related by the expression

$$v_0 S(S+1) / \left(4\pi \int_0^\infty r^2 \gamma(r) dr \right) = (\kappa_1 r_1)^2 = \chi_1 / \chi, \quad (18)$$

where, as before, χ_1 is the paramagnetic susceptibility for noninteracting spins and χ is the observed susceptibility. The length r_1 is expected to vary slowly with temperature compared with κ_1 , and must be of microscopic size. This last follows since for T/T_c considerably greater than one, χ_1/χ approaches unity, and κ_1^{-1} approaches r_1 . Since the range of the correlations must be of microscopic size at these high temperatures, r_1 must be of the order of interatomic spacings. (The fact that Eqs. (17) and (18) are not expected to hold quantitatively for temperatures far removed from T_c should not effect this order of magnitude argument.) In contrast to the expected behavior of r_1 , κ_1 must approach zero as $T \rightarrow T_c$ and $\chi \rightarrow \infty$.

Numerical estimates for the temperature region of validity of Eq. (17) are easily obtained. Derivation of Eqs. (17) and (18) supposes that the fractional change in $\gamma(r)$ over a lattice spacing is small, so that the discrete correlation function may be treated as continuous, and the true $\gamma(r)$ replaced by its asymptotic value. If a_0 is the nearest neighbor separation ($a_0 = 2.48$ Å for α -iron) this evidently requires that

$$\kappa_1 a_0 \ll 1, \quad (19)$$

or

$$\kappa_1 a_0 \lesssim \frac{1}{10}.$$

This restriction on the range κ_1^{-1} of the correlations may be expressed as an upper limit on the temperature region

⁶ L. S. Ornstein and F. Zernike, Proc. Acad. Sci. Amsterdam 17, 793 (1914); Physik. Z. 19, 134 (1918).

of validity. From Eq. (18) using the experimentally⁷ observed χ and putting $r_1 \approx a_0$ we have the estimate

$$T - T_c \lesssim 25^\circ. \quad (20)$$

This rather small temperature interval would be significantly increased by a somewhat larger upper bound for κ_1 . For example, if we use $\kappa_1 a_0 \lesssim \frac{1}{5}$, then the temperature interval is about four times larger than that given by Eq. (20). Since the temperature region is only roughly estimated by this procedure, we will see to what extent the $\gamma(r)$ determined by Fourier inversion exhibit the asymptotic behavior expressed by Eq. (17), even though the temperature interval spanned by the experimental data is larger than given by Eq. (20).

If the $\gamma(r)$ obtained in the previous section has the behavior expressed by Eq. (17), then a plot of $\log[r\gamma(r)]$ against r should be a straight line with slope $-\kappa_1$ and intercept at $r=0$ of $v_0 S(S+1)/(4\pi r_1^2)$. Figure 5 shows that the correlations at larger distances do indeed exhibit this behavior. From the straight lines drawn in the figure, the values of r_1 and κ_1^{-1} listed in Table II are obtained. Also given are estimates of the precision of the results so obtained. From the table one sees that the quantity, κ_1^{-1} , which measures the range of the correlations, decreases rapidly with increasing temperatures close to the Curie point, followed by a more gradual decrease as the temperature is further increased. The length r_1 decreases rather slowly with increasing temperature, a behavior to be expected from detailed considerations involved in the derivation of the asymptotic form.

In Table III, the asymptotic $\gamma(r)$ are compared with the values obtained from Fourier inversion. For distances larger than about 6 Å, the agreement between the two is quite good. At shorter distances, the asymptotic expression gives $\gamma(r)$ values considerably higher than those obtained from Fourier inversion. This result is, of course, a consequence of the functional form of the asymptotic expression.

These results for $\gamma(r)$ will now be compared with the observed susceptibility according to Eq. (18),

$$v_0 S(S+1)/I = (\kappa_1 r_1)^2 = \chi_1/\chi,$$

where

$$I = 4\pi \int_0^\infty r^2 \gamma(r) dr.$$

TABLE II. Values of κ_1^{-1} and r_1 obtained from the straight-line fit to the curves of $\log r\gamma(r)$ versus r .

T (°C)	κ_1^{-1} (Å)	r_1 (Å)
754	34.8 ± 6.5	1.05 ± 0.05
790	6.8 ± 0.7	1.05 ± 0.04
836	4.3 ± 0.3	0.91 ± 0.04
854	3.2 ± 0.1	0.74 ± 0.03

⁷ The data used are those of L. Néel, Ann Physik 18, 5 (1932) and H. H. Potter, Proc. Roy. Soc. (London) A146, 362 (1934).

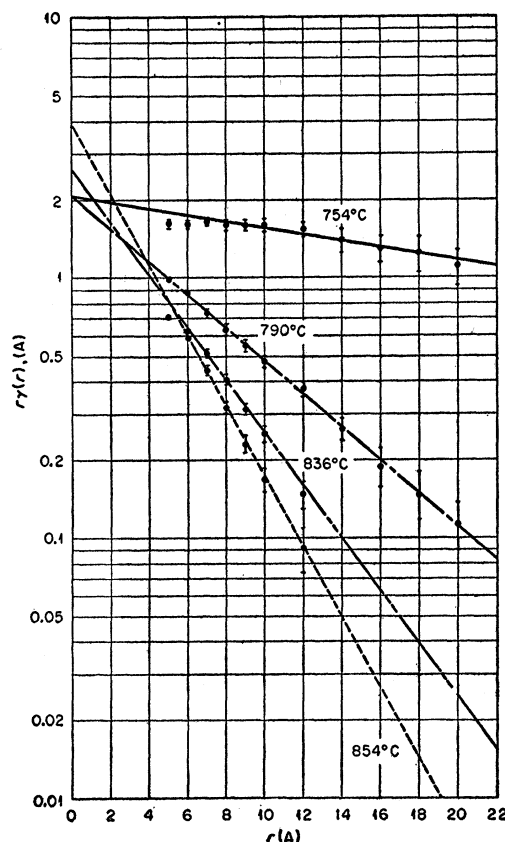


FIG. 5. Dependence of $r\gamma(r)$ on distance r at different temperatures.

In calculating the space integral of the correlations, the contributions from r greater than 20 Å, which is the maximum distance covered by the Fourier inversion, are by no means negligible. For these distances the asymptotic forms for $\gamma(r)$ have been used. In Table IV we list separately the contributions to the integral I from the two distance ranges. Their sum is then used to determine the ratio $(\chi_1/\chi)_{\text{exp}}$ as obtained from the small-angle neutron scattering. The same value should result from the quantity $(\kappa_1 r_1)^2$ so long as replacing $\gamma(r)$ everywhere by its asymptotic form is a good approximation, i.e., when the range of the correlations is sufficiently great. A comparison of $(\chi_1/\chi)_{\text{exp}}$ with $(\chi_1/\chi)_{\text{asympt}}$ in Table IV shows that this condition is fulfilled at the two lowest temperatures. For the highest two temperatures, however, the asymptotic form for $\gamma(r)$ gives too large a value for the space integral and hence too small a value for the ratio $(\chi_1/\chi)_{\text{asympt}}$.

In the last column of the table we give the values for the ratio $(\chi_1/\chi)_{\text{mag}}$ with χ obtained from magnetic measurements. It appears that for temperatures in the neighborhood of the Curie point, these values are not precisely known. Néel⁷ has made detailed measurements of χ in the range of temperatures from the Curie point at 770°C up to 800°C. His results show that the value

TABLE III. Comparison of $\gamma(r)$ obtained from Fourier inversion with asymptotic expression $\gamma(r)_{\text{asympt}}$.

r (Å)	754°C		790°C		836°C		854°C	
	$\gamma(r)$	$\gamma(r)_{\text{asympt}}$	$\gamma(r)$	$\gamma(r)_{\text{asympt}}$	$\gamma(r)$	$\gamma(r)_{\text{asympt}}$	$\gamma(r)$	$\gamma(r)_{\text{asympt}}$
2	0.495	0.986	0.371	0.779	0.274	0.830	0.280	1.070
4	0.368	0.466	0.255	0.290	0.187	0.260	0.190	0.286
6	0.276	0.293	0.146	0.144	0.105	0.108	0.0984	0.102
8	0.200	0.208	0.0795	0.0810	0.0510	0.0512	0.0398	0.0408
10	0.161	0.157	0.0481	0.0481	0.0256	0.0255	0.0168	0.0175
12	0.129	0.123	0.0315	0.0298	0.0124	0.0133	0.0077	0.0078
14	0.101	0.100	0.0188	0.0191	0.00218	0.0073	0.0024	0.0036
16	0.081	0.082	0.0117	0.0124	...	0.0039	...	0.0016
18	0.070	0.069	0.0073	0.0082	...	0.0022	...	0.0008
20	0.056	0.059	0.0056	0.0055	...	0.0012	...	0.0004

for χ at a particular temperature is changed by about 25% by cooling the iron sample and reheating. The measurements of Potter⁷ which extend from the Curie point up to 840°C give $1/\chi$ values larger than Néel's average values by about 30%. The data of Sucksmith and Pearce⁸ which go down to 824°C yield $1/\chi$ values about 30% smaller than Potter's in the overlap region. The values $(\chi_1/\chi)_{\text{mag}}$ given in Table IV are averages of the experimental results with errors estimated from differences between independent results. In obtaining these values, the temperature scale has been readjusted to shift the Curie point to 760°C, the temperature at which the observed neutron scattering at fixed small angle is a maximum (Fig. 3). Considering the uncertainty in the experimental susceptibilities as well as the uncertainty in the adjustment of the temperature scales, the comparison of the quantity χ_1/χ obtained from the two methods appears to be quite satisfactory.

V. CONCLUSIONS

Fourier analysis of the small-angle magnetic scattering of 0.9 Å neutrons by iron in the vicinity of the Curie point yields the behavior of the instantaneous correlation between pairs of spins of the iron atoms. These correlations are found to be monotonic decreasing functions of the distance between atoms, with a range which rapidly increases as the temperature approaches the Curie point. For temperatures up to about 90°C above the Curie temperature, the pair correlations appear to have the asymptotic behavior predicted by statistical mechanics. The volume integral of the pair correlation function yields values for the susceptibility of iron which are consistent with the measured values.

TABLE IV. Comparison between values for (χ_1/χ) predicted from magnetic neutron scattering with $(\chi_1/\chi)_{\text{mag}}$ obtained from susceptibility measurements.

T (°C)	$r \leq 20\text{Å}$ (Å ³)	$r \geq 20\text{Å}$ (Å ³)	$(\chi_1/\chi)_{\text{exp}}$ ($\times 10^{-4}$)	$(\chi_1/\chi)_{\text{asympt}}$ ($\times 10^{-4}$)	$(\chi_1/\chi)_{\text{mag}}$ ($\times 10^{-4}$)
754	279	2245	9 ± 2	9	8.5 ± 2
790	71	20	242 ± 30	238	150 ± 30
836	39	3	530 ± 70	454	390 ± 40
854	31	...	700 ± 90	536	480 ± 30

⁸ W. Sucksmith and R. R. Pearce, Proc. Roy. Soc. (London) **A167**, 189 (1938).

ACKNOWLEDGMENTS

We wish to express our appreciation to A. W. McReynolds, T. Riste, L. Van Hove, and E. O. Wollan for helpful conversations. One of us (H.A.G.) wishes to express his appreciation to the Oak Ridge Institute of Nuclear Studies and to the Physics Division of the Oak Ridge National Laboratory for their hospitality during the summer of 1955.

APPENDIX I. RELATION BETWEEN MAGNETIC MOMENT FLUCTUATIONS AND CORRELATIONS BETWEEN PAIRS OF SPINS

The magnetic moment of the region Ω containing N_Ω spins is

$$\mathbf{M}_\Omega = -2\beta \sum_{i=1}^{N_\Omega} \mathbf{S}_i, \quad (\text{AI.1})$$

where β is the Bohr magneton.

The mean square deviation of the fluctuations in M_Ω from the average will be given by

$$\begin{aligned} \langle M_\Omega^2 \rangle - |\langle \mathbf{M}_\Omega \rangle|^2 &= 4\beta^2 \langle \sum_i \mathbf{S}_i \cdot \sum_j \mathbf{S}_j \rangle - 4\beta^2 \langle \sum_i \mathbf{S}_i \rangle^2 \\ &= 4\beta^2 N_\Omega \langle S^2 \rangle - 4\beta^2 N_\Omega^2 S_T^2 \\ &\quad + 4\beta^2 \sum_{i \neq j} \langle \mathbf{S}_i \cdot \mathbf{S}_j \rangle, \end{aligned} \quad (\text{AI.2})$$

where $\langle S^2 \rangle$ and S_T^2 are single-spin averages, $\langle S^2 \rangle = S(S+1)$, with S the atom spin quantum number and $\mathbf{S}_T = N_\Omega^{-1} \langle \sum_i \mathbf{S}_i \rangle$ is the average spin vector per atom.

Now separate out the asymptotic value of $\langle \mathbf{S}_i \cdot \mathbf{S}_j \rangle$ by writing

$$\begin{aligned} \langle \mathbf{S}_i \cdot \mathbf{S}_j \rangle &= S_T^2 + \{ \langle \mathbf{S}_i \cdot \mathbf{S}_j \rangle - S_T^2 \} \\ &= S_T^2 + \gamma_{ij}'. \end{aligned} \quad (\text{AI.3})$$

Then Eq. (AI.2) may be written in the form

$$\begin{aligned} \langle M_\Omega^2 \rangle - |\langle \mathbf{M}_\Omega \rangle|^2 &= 4\beta^2 N_\Omega [S(S+1) - S_T^2] + 4\beta^2 \sum_{i \neq j} \gamma_{ij}'. \end{aligned} \quad (\text{AI.4})$$

Our discussion in Sec. II has shown that at temperatures removed from the Curie point, fluctuations are normal, and the quantity $\langle M_\Omega^2 \rangle - |\langle \mathbf{M}_\Omega \rangle|^2$ is proportional to N_Ω . From Eq. (AI.4), we see that this requires

γ_{ij}' , which depends on the distance between the i th and j th spins, to decay to zero over distances small compared with $\Omega^{\frac{1}{2}}$ so that the double sum may be written in the form

$$\sum_{i \neq j} \gamma_{ij}' = N_{\Omega} \sum_{R \neq 0} \gamma_{R}', \quad (\text{AI.5})$$

where the sum on the right side gives a value independent of N_{Ω} . As T approaches T_c , since fluctuations become tremendous, $\langle M_{\Omega}^2 \rangle - |\langle \mathbf{M}_{\Omega} \rangle|^2$ must become proportional to a higher power of N_{Ω} , and this fact requires γ_{ij}' to decay very slowly so that it is still appreciable for separation distances of order $\Omega^{\frac{1}{2}}$.

APPENDIX II. ESTIMATE OF THE DEGREE OF INELASTICITY IN THE MAGNETIC NEUTRON SCATTERING

In this Appendix, we give some estimates to show the validity of the approximation of negligible neutron energy exchange with the spin lattice in the range of the experimental conditions. These estimates are based on the treatment of the time dependent correlations given by Van Hove.³ The asymptotic form for the pair correlation function for times considerably greater than microscopic relaxation times as given by Eq. (38) of reference 3 is

$$\gamma_{R'}(t) = (4\pi r_1^2)^{-1} v_0 S(S+1) (4\pi \Lambda_1 |t|)^{-\frac{3}{2}} \times \int \exp\left\{ \frac{-|\mathbf{R}-\mathbf{R}'|^2}{4\Lambda_1 |t|} - \kappa_1 R' \right\} \frac{d\mathbf{R}'}{R'}, \quad (\text{AII.1})$$

where r_1 and κ_1^{-1} are the lengths characterizing the instantaneous correlation

$$\gamma_{R'}(0) = (4\pi r_1^2 R)^{-1} v_0 S(S+1) \exp(-\kappa_1 R), \quad (\text{AII.2})$$

and where $\Lambda_1 = \lambda/\chi$, χ being the observed susceptibility and λ a phenomenological constant. The significance of Λ_1 is that it measures the time decay of a plane wave fluctuation of the magnetic moment, the time decay being given by $\exp(-\Lambda_1 k^2 t)$, where \mathbf{k} is the wave vector. When $T \rightarrow T_c$, $\Lambda_1 \rightarrow 0$, since then $\chi \rightarrow \infty$ and λ is expected to vary only slowly with T . Our aim is to show that for our experimental conditions Λ_1 is sufficiently small to justify the static approximation.

When the time-dependent correlation given by Eq. (AII.2) is inserted in our Eq. (3), one gets for the differential cross section for inelastic magnetic scattering the expression

$$\frac{d^2\sigma}{d\Omega d\epsilon} = \left(\frac{\gamma e^2}{mc^2} \right)^2 \frac{2N}{3\pi\hbar} S(S+1) \frac{k}{k_0} |f(\kappa)|^2 \times \sum_{\boldsymbol{\tau}} \frac{1}{r_1^2 \{ |\boldsymbol{\kappa}-\boldsymbol{\tau}|^2 + \kappa_1^2 \}} \frac{\Lambda_1 |\boldsymbol{\kappa}-\boldsymbol{\tau}|^2}{\Lambda_1^2 |\boldsymbol{\kappa}-\boldsymbol{\tau}|^4 + \omega^2}. \quad (\text{AII.3})$$

Here the sum is over the vectors $\boldsymbol{\tau}$ of the reciprocal lattice. As before, the terms in the sum corresponding

to $\boldsymbol{\tau} \neq 0$ may be neglected for the small-angle magnetic scattering with which we are concerned. Integrating over final neutron energy, we have

$$\frac{d\sigma}{d\Omega} = \left(\frac{\gamma e^2}{mc^2} \right)^2 \frac{2N\hbar S(S+1)}{3\pi m k_0} |f(\kappa)|^2 \times \int \frac{k^2 dk}{r_1^2 \{ \kappa^2 + \kappa_1^2 \}} \frac{\Lambda_1 \kappa^2}{\Lambda_1^2 \kappa^4 + \omega^2}, \quad (\text{AII.4})$$

where the form factor f^2 has been removed from the integral since we will be considering only small κ values. Making the substitutions $\alpha = (k - k_0)/k_0$, $\delta = m\Lambda_1/\hbar$, $\beta = \kappa_1/k_0$, and putting $\sin\theta = \theta$, this equation becomes

$$\frac{d\sigma}{d\Omega} = \frac{2N}{3} \left(\frac{\gamma e^2}{mc^2} \right)^2 S(S+1) \frac{|f(\kappa)|^2}{\pi r_1^2 k_0^2} \times \int (1+\alpha)^2 d\alpha \left[\frac{1}{\alpha^2 + \theta^2 (1+\alpha) + \beta^2} \right] \times \left\{ \frac{\delta [\alpha^2 + \theta^2 (1+\alpha)]}{\delta^2 [\alpha^2 + \theta^2 (1+\alpha)]^2 + \alpha^2 (1 + \frac{1}{2}\alpha)^2} \right\}. \quad (\text{AII.5})$$

If we had used instead the static approximation $\gamma_{R'}(0)$, we would have obtained

$$\frac{d\sigma}{d\Omega} = \frac{2N}{3} \left(\frac{\gamma e^2}{mc^2} \right)^2 S(S+1) \frac{|f(\kappa)|^2}{r_1^2 k_0^2} \frac{1}{\theta^2 + \beta^2}. \quad (\text{AII.6})$$

Comparing the last two equations, we see that the static approximation will be a good one whenever the spread in the length of the final momentum caused by energy exchanges and represented by the half-width of the term in curly brackets in Eq. (AII.5) is much less than the momentum transfers represented by the half-width of the term in square brackets. Solving for these half-widths, we have

$$\left\{ \frac{1}{2\delta^2} [1 + (2\delta^2\theta^2)^2]^{\frac{1}{2}} - \frac{1}{2\delta^2} \right\}^{\frac{1}{2}} \lesssim \frac{1}{10} (\theta^2 + \beta^2)^{\frac{1}{2}}, \quad (\text{AII.7})$$

as the requirement for negligible energy exchange. This condition is equivalent to a restriction on two characteristic times. Recalling that $\delta \rightarrow 0$ as $T \rightarrow T_c$, we may suppose that $2\delta^2\theta^2 \ll 1$, so that Eq. (AII.7) becomes

$$\delta\theta^2 \lesssim \frac{1}{10} (\theta^2 + \beta^2)^{\frac{1}{2}}, \quad (\text{AII.8})$$

or

$$\Lambda_1 \kappa^2 \lesssim \frac{1}{10} v (\kappa^2 + \kappa_1^2)^{\frac{1}{2}},$$

where v is the neutron velocity, and $\kappa^2 = k_0^2 \theta^2$. Since a plane wave fluctuation in the magnetic moment decays like $\exp(-\Lambda_1 k^2 t)$, the quantity $\Lambda_1 \kappa^2$ on the left above is the reciprocal of t_0 , the decay time of the plane wave fluctuation with which the neutron interacts when the momentum transfer is $\hbar\kappa$. On the right side, neglecting the factor κ^2 , we have $\kappa_1 v$, the reciprocal of the time t'

that the neutron spends in the correlation range κ_1^{-1} . Hence Eq. (AII.8) may be written as

$$t_0 \gtrsim 10t'. \quad (\text{AII.9})$$

This relation shows that for negligible energy exchange, the relaxation time for the magnetic moment fluctuations should be much greater than the time spent by the neutron in traveling over a correlation range. The temperature dependence of the time t' is easily obtained from the relation $(\kappa_1 r_1)^2 = \chi_1/\chi$, giving

$$t' = (r_1/v)(\chi/\chi_1)^{1/2}. \quad (\text{AII.10})$$

The time $t_0 = (\Delta_1 \kappa^2) = \chi/(\lambda \kappa^2)$ may be estimated from the fact that at high temperatures t_0 becomes a microscopic relaxation time which has been calculated³ to be about $20\hbar/J$, where J is the interaction energy between a pair of spins. For $T/T_c \gg 1$, $\chi \rightarrow \chi_1$, the paramagnetic susceptibility for noninteracting spins. Also, the im-

portant momentum transfers must be of order \hbar/r_1 , since r_1 then represents the range of the correlations. This determines the phenomenological constant λ and, assuming it to be temperature-independent, gives for the relaxation time t_0 the estimate

$$t_0 \cong (20\hbar/Jr_1^2\kappa^2)(\chi/\chi_1). \quad (\text{AII.11})$$

(The fact that we have here extrapolated results valid near T_c and for long times to much higher temperatures and microscopic times should not affect the order of magnitude of the results.) Our requirement for negligible energy exchange now reads

$$(20\hbar/Jr_1^2\kappa^2)(\chi/\chi_1) \gtrsim 10(r_1/v)(\chi/\chi_1)^{1/2}. \quad (\text{AII.12})$$

Inserting the pertinent values, one sees that this condition is certainly fulfilled over the temperature range we have used and over the values for $\kappa = k_0\theta$ corresponding to the small angles involved.

Relaxation Time of Surface States on Germanium*

R. H. KINGSTON AND A. L. MCWHORTER

Lincoln Laboratory, Massachusetts Institute of Technology, Lexington, Massachusetts

(Received March 5, 1956)

Two types of state exist at the surface of single crystal germanium; the first type, which is assumed to be at the semiconductor-oxide interface, is chiefly responsible for the carrier recombination process, while the second type, associated with the oxide structure and adsorbed ions, is believed to control the position of the Fermi level at the surface with respect to the electron band energy. The latter type of state has been studied by means of the "field-effect," or change in conductance with an applied field perpendicular to the surface. The results indicate that the relaxation or capture time of these states is much longer than that of the interface states, and is also extremely sensitive to surface treatment and ambient gas. In addition, some surface treatments lead to a distribution of time constants on the same surface over a range as large as six decades. Possible physical models for this behavior are discussed as well as its connection with excess or $1/f$ noise.

INTRODUCTION

EARLY in the study of high-purity germanium as a semiconductor, it became apparent that the surface of the material had additional energy states for electrons beyond those normally expected in the bulk material. In particular, it was necessary to postulate electron levels in the gap both to explain metal-semiconductor rectification¹ and later to explain surface recombination velocity.² Direct evidence for the existence of such states was found by Shockley and Pearson,³ who attempted to modulate the conductivity of a thin evaporated film of germanium by applying an

external electric field normal to the surface. Since the change in conductivity was only about 10% of what had been expected from the magnitude of the induced charge and the free carrier mobility, it was necessary to assume that there were localized levels at the surface which would absorb and thereby immobilize the majority of the induced charge. Recently, this experiment, the "field effect," has been studied in more detail on single crystal germanium slabs⁴⁻⁹; and, in conjunction with measurements of surface conductance on

* The research reported in this document was supported jointly by the Army, Navy, and Air Force under contract with the Massachusetts Institute of Technology.

¹ J. Bardeen, *Phys. Rev.* **71**, 717 (1947).

² W. H. Brattain and J. Bardeen, *Bell System Tech. J.* **32**, 1 (1953).

³ W. Shockley and G. L. Pearson, *Phys. Rev.* **74**, 232 (1948).

⁴ J. Bardeen and S. R. Morrison, *Physica* **20**, 873 (1954).

⁵ G. G. E. Low, *Proc. Phys. Soc. (London)* **B68**, 10 (1955); **B68**, 1154 (1955).

⁶ R. H. Kingston and A. L. McWhorter, *Phys. Rev.* **98**, 1191 (1955).

⁷ W. L. Brown, *Phys. Rev.* **98**, 1565 (1955); **100**, 590 (1955).

⁸ H. C. Montgomery and W. L. Brown, *Phys. Rev.* **98**, 1565 (1955).

⁹ S. G. Kalashnikov and A. E. Yunovich, *J. Tech. Phys. (U.S.S.R.)* **25**, 952 (1955).